Experimental and Numerical Analysis of Faulty Operation of a Superconducting Solenoid Made of Tape with High Temperature Superconductor

Blazej Skiba[1,a)], Lukasz Tomkow[2], Evgeniy Kulikov[3], Valeriy Drobin[3] and Ziemowit Malecha[1]

[1]*Faculty of Mechanical and Power Engineering, Wroclaw University of Technology, Wroclaw, Poland*
[2]*Department of Materials Science and Metallurgy, University of Cambridge, Cambridge, United Kingdom*
[3]*Laboratory for High Energy Physics, Joint Institute for Nuclear Research, Dubna, Russia*

[a)]Corresponding author: skiba.blazej@yahoo.com

Abstract. Superconducting magnets allow to obtain high magnetic fields. The application of tapes with high temperature superconductors enables them to operate in liquid nitrogen, thus decreasing overall cost of operation. However, ceramic structure of the tapes is prone to mechanical damages decreasing critical current density.
This works presents the results of the analysis of the operation of a superconducting magnet. Preliminary design considerations and expected performance are calculated numerically. The experimental results show the degeneration of the structure of the tape. Possible causes of faulty operation and available remedies are discussed.

INTRODUCTION

The applications of second generation (2G) tapes with high temperature superconductors (HTS) are becoming increasingly popular. They are used for fabricating the magnets used in many fields, including power industry, transport, medicine, high energy physics and many others.
HTS materials are a hope for improvement of operation of superconducting magnetic energy storage (SMES) systems. Research shows that HTS designs have reduced volumes compared to designs with low temperature supercondicting (LTS) NbTi coils [1]. HTS magnets for 2.5 MJ SMES are designed [2]. The HTS current leads from Bi-2223 AgAu matrix tapes are developed and successfully tested for ITER megaproject [3]. This may allow reducing the cryoplant capacity by 25%. For future devices, there exists a possibility of introducing magnets made of HTS. It provides an opportunity for reduced maintenance or lowers costs [4] and for achieving magnetic fields above 20 T [5]. HTS are able to produce strong magnetic levitation forces with designed for magnetic levitation transportation systems [6]. New dynamo-type HTS flux pumps are developed for injecting a DC into a circuit with superconductors without currents leads [7]. Recently, jointless HTS solenoids are designed and fabricated [8]. Different methods for charging up such magnets are tested.
HTS is prominent technology for future high magnetic field applications. HTS 2G tapes are developed for magnets in colliders e.g. for muon colliders in Small Business Innovative Research series [9] or for dark matter search experiments [10]. LTS magnets for ECR ion sources are limited to frequencies of 28 GHz for NbTi, and of about 56 GHz for Nb_3Sn, while HTS systems could achieve even 84 GHz. Superconducting joints made of REBCO wires are developed and tested for MRI magnets [11]. Cryogen-free 9,4 T HTS magnet is tested for purpose of nuclear magnetic resonance [12].
Main reason for HTS quenching is non-ideality of a conductor or manufacturing process of a coil [13]. Due to low quench propagation velocities the active protection systems have to be used [14]. Different new ways of quench protection are considered to ensure operation of HTS coils, e.g. reducing hot-spot temperatures in sub-coils [15]. Damages of HTS tapes are caused by the fracture of the cores induced by the excessive straining [16]. For optimal design of solenoids particle swarm optimisation algorithm combined with finite-element may be used [17].

A superconducting solenoid made of tape with high temperature superconductor (HTS) is investigated. Its purpose is to create a magnetic field during a research concerning the utilisation of open-type superconducting magnetic shield for improving the uniformity of magnetic field. Experiments are conducted in the Joint Institute for Nuclear Research (JINR), in Dubna (Russia), in Veksler and Baldin Laboratory of High Energy Physics (VBLHEP). The primary motivation behind them is the application of an open-type superconducting shields for an electron cooling system. The system will be the part of the Booster of NICA complex, which is currently under construction at JINR. The main iam of the NICA complex is to search for possible mixed phase state and potential critical points of the transition of phases [18]. The proposed solution for the Booster is described at [19].
The aim of this paper is to present the numerical and experimantal analysis of the operation of the superconducting solenoid. The results show that faults decrease critical current of the superconducting tape and the tests of the solenoid exacerbated the problem. Possible reasons of such behaviour are discussed along with available remedies.

METHODS

Experimental

SCS12050 tape made by SuperPower is used to wound the solenoid. The producer declares critical current of the tape in self-field as 300 A. The critical bend diameter of the tape is 25 mm. The solenoid is equipped with some safety mechanisms intended to decrease negative effects of the quench. Parallelly to the magnet a warm diode and an external dump resistor are connected to route an exceed electric current out of the solenoid.
The investigated solenoid is placed in the cryostat. The cryostat is made from a non-magnetic stainless steel. It is filled with liquid nitrogen. The cryostat is vacuum-insulated to reduce the heat in leaks to the cryogen, thus reduce its losses due to boiling. The bottom of the cryostat was insulated with a foamed polystyrene.The current to the magnet is supplied through the normal conducting power leads from the American Magnetics power DC power supply AMI 12200PS. The voltage drop is measured by the Keithley Naptech 63538. The cryostat is equipped with a warm tunnel for introducing the magnetic field measuring probe during latter experiments.
At figure 1 the cryostat is presented. On segment I, the assembled cryostat with electrical connections is presented, on segment II, the cold head during the experiments, on segment III the inside view. The vent (A) is the warm tunnel for introducing the measuring probe. The hole (B) is for placing the magnet. On the surface (C), the superconducting magnetic shielding is located.
For the current up to 10 A, measurements is taken every 1 A, to make an initial check of the magnet. Then the density of the measurement is lowered. The ramp-up of the current is slow to precisely obtain the desired value and to prevent increasing the current above the safe value. It would create a risk of a large quench at the solenoid. Between each measurement a short pause is made to ensure the proper readout of the voltage drop. This is to relax the losses due to the varying current inducing electric field in the superconductor. This could lead to falsified read of the voltage drop, which does not occur during the normal DC conditions.

Numerical

Numerical model is developed to predict the critical current of the electromagnet and assess its changes. It uses Magnetic Fields interface from AC/DC package of Comsol Multiphysics numerical software. Axial symmetry of the solenoid is explotied to decrease the size of the model and computation. A dense mesh is applied with typical size of element at the order of 10 μm. The mesh is presented in figure 2a. Magnetic insulation boundary condition is imposed on the external borders of the model region. Axial symmetry condition is used where applicable. To model the current in the electromagnet external current density is used, which assumes that the current flow uniformaly in the volume of the solenoid. Relative magnetic permeability of all regions of the model is assumed to be 1. The summary of the applied boundary conditions is also presented in figure 2b.
After obtaining the magnetic field distribution the corresponding critical current density J_c in the magnet region is found. The method to find J_c is based on the equations and parameters from [20]. The model assumes a simple proportional power law in which critical current density is proportional to the local magnetic induction according to formula 1.

$$J_c \propto B^{-n} \tag{1}$$

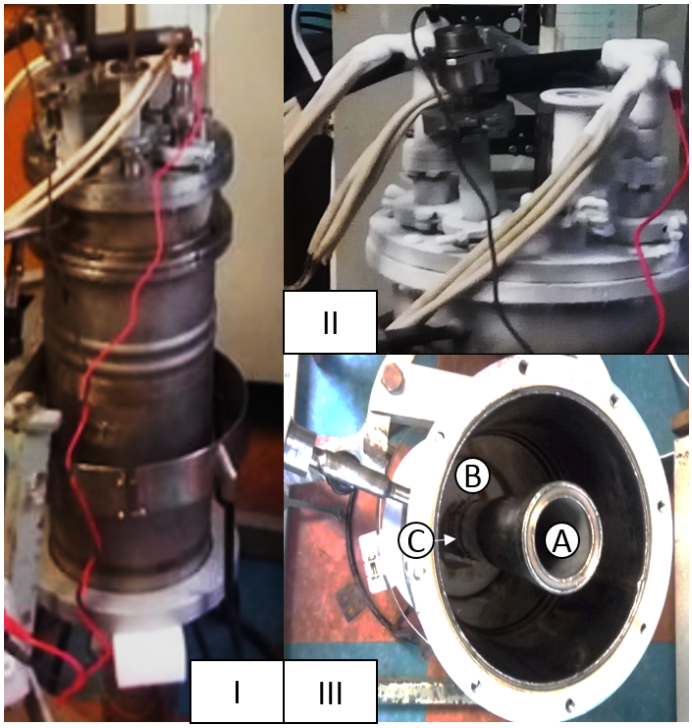

FIGURE 1: The cryostat used for the experiments: I - assembled, II - cold head during the operation, III - inside view

n is the exponent of power law for electric current density calculations. The exact formula used in model is shown below (2).

$$J_c = J_0 \cdot \frac{B^{-n}}{B_0^{-n}} \tag{2}$$

In this formula J_0 is critical current density given at B_{ref}, a certain magnetic reference magnetic induction depending on available material data. [20] gives the value of $8 \cdot 10^9\ A/m^2$ for J_0 and 0.01 T for B_{ref}. n is 0.75, according to material data for SuperPower tapes used in experimental part.
By combining the results from the numerical model and analytical formulas graph 5 is created showing the dependence of critical current density on magnetic induction and the maximum and desired magnetic induction obtained with magnet at the given current. The cross between the values of maximum magnetic induction and critical current marks an expected quench field and current.

RESULTS AND DISCUSSION

Figure 3a shows the distribution of magnetic field expected in the moment of quench during the design of the magnet. The maximum achievable field of the magnet is supposed to be almost 3 T with the applied current of slightly more than 130 A. In this case current density in the magnet is equaly to critical current as seen in figure 3b. Due to the fault such performance of the magnet is not achieved.

Figure 4 presents the measured current-voltage characteristic. Although the magnet is initially in superconducting state a certain voltage drop is observed. The voltage drop ise due the normal conducting elements of the circuit. Current-voltage characteristic below 20 A is linear. The slope of the curve obtained in this range is 1.69. At about 20.5 A, the voltage drop drastically increases, meaning the some domains of the magnet return to the normal state.
In further experiments the applied current of 20 A is not exceeded. The magnetic field generated at the applied current of 20 A is approximately 0.5 T. During the further measurements the measured charactestics differ from the ones obtained initially. The new voltage drops were significantly higher. Both characteristics are presented in figure 4. The slope after the quench is 40.9500.

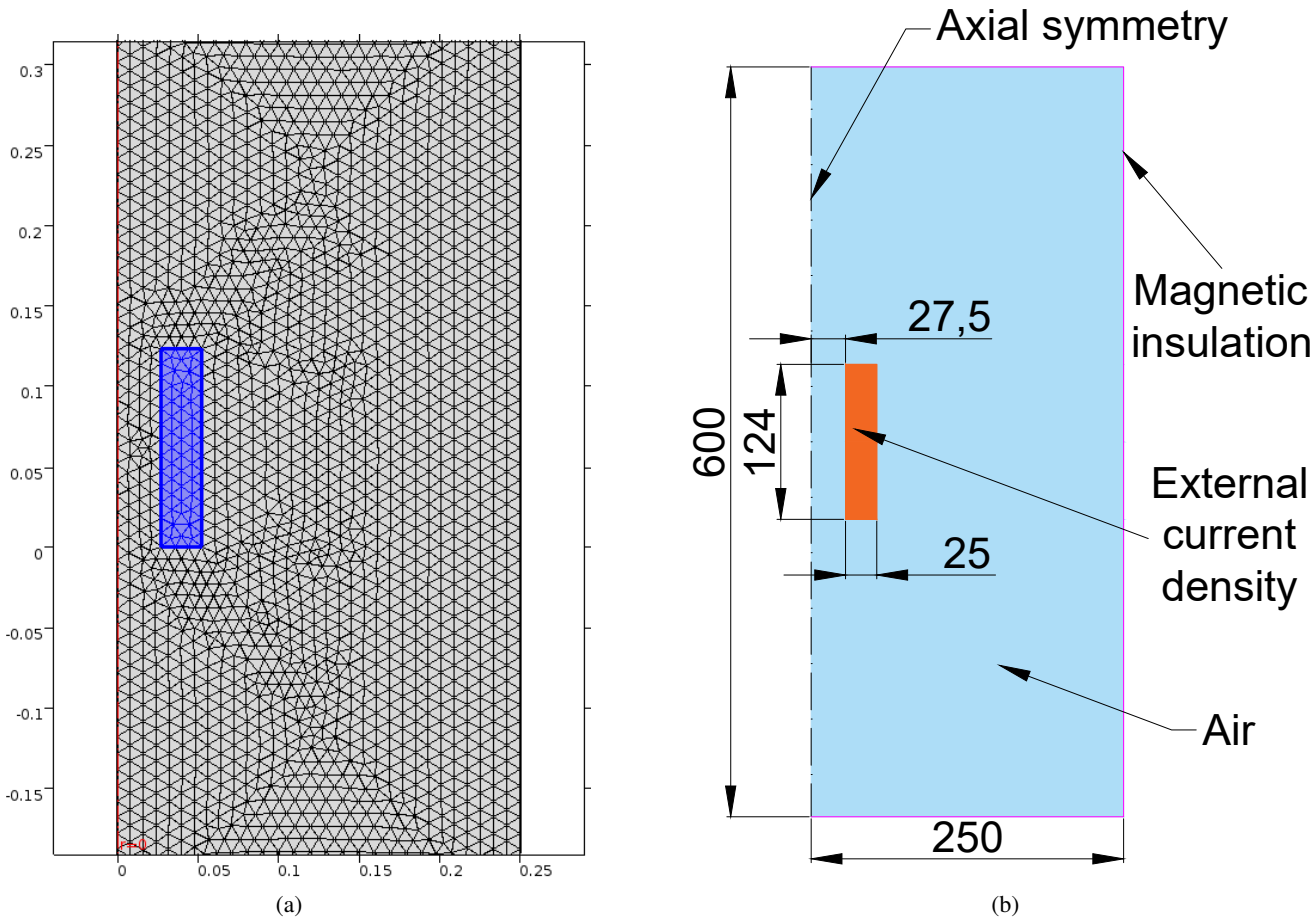

(a) (b)

FIGURE 2: (a) Numerical mesh with the solenoid marked in blue; (b) boundary conditions used in the numerical calculations

Several rounds of experiments are performed to further analyse the fault. The magnet is ensured to be cooled down enough to eliminate possibility of non-uniform cooling. To further decrease AC losses the ramp of the applied current is even lower. The auxiliary devices are examined to find the source of the observed problems. The external dump resistor is disconnected from the circuit to ensure it does not falsify the measurements.

A new measuring system is assembled with a new power source. After all these improvement the problem with high voltage drops persists and it can be concluded that the solenoid is damaged. The visual examination of the magnet did not show any possible damaged areas. There are no visible hot spots or other damages. Current leads, feeding the magnets, are reinforced by the addition of the Kapton tape as it was the most probable area for the failure of the magnet.

However, the tape in the region of current leads is bent at small diameter. HTS tapes are very sensitive to bending and fragile. It is possible that they were damaged during manufacturing and the ceramic structure of the superconductor lost its continuity. The degradation of critical current is well visible in figure 5. The critical current observed in the assembled solenoid is more than 5 times lower than expected and so is the achieved magnetic field. After initial test the superconducting tape degraded further to the point of full breakage of the superconducting layer.

Three mechanisms may lead to further damage and be responsible for rendering the magnet useless. The first is the thermal shock occuring during rapid cooldown with liquid nitrogen. Secondly, mechanic breakage during the placement of the magnet or due to Lorentz forces can strain the tape. Finally, the local hot stop can lead to uncontrolled temperature growth.

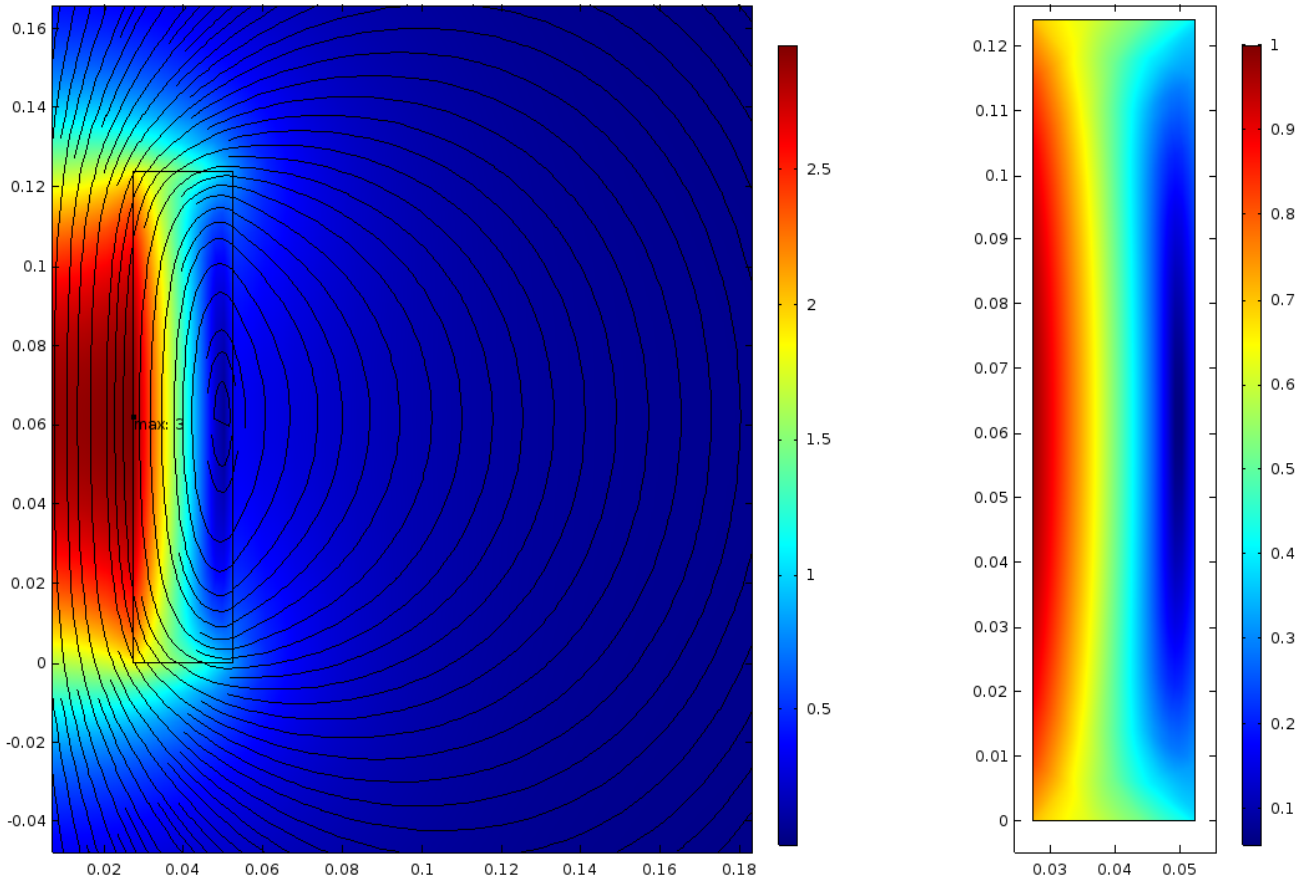

(a) (b)

FIGURE 3: (a) Magnetic induction generated by the magnet in T with applied current of 132 A; (b) Ratio between J and J_c with applied current of 132 A

The resistivity of the magnet is measured locally to find possible effects of the quench. The HTS coil retains the resistivity in the measured areas - no local disturbance in the value of measured parameters are found. Further works will be performed to refurbish the magnet which will require its partial unwinding and removal of the damaged sections of the tape. The presented results show that special care and additional precautions should be always taken when working with the superconducting tape. The most sensitive piece of the device are current leads which should be designed to minimise the required bending and maximise the bending radius.

CONCLUSIONS

The results of the analysis show that the critical current of the superconducting solenoid is degraded. During the initial test the quench occured too early. In further measurements sections of the magnet remained in normal state. The fault is probably located in current leads. Too small bending radius lead to damage and further destruction of the tape. The redesign and replacement of the current leads is necessary to resume the operation of the magnet with nominal parameters predicted with the numerical model.

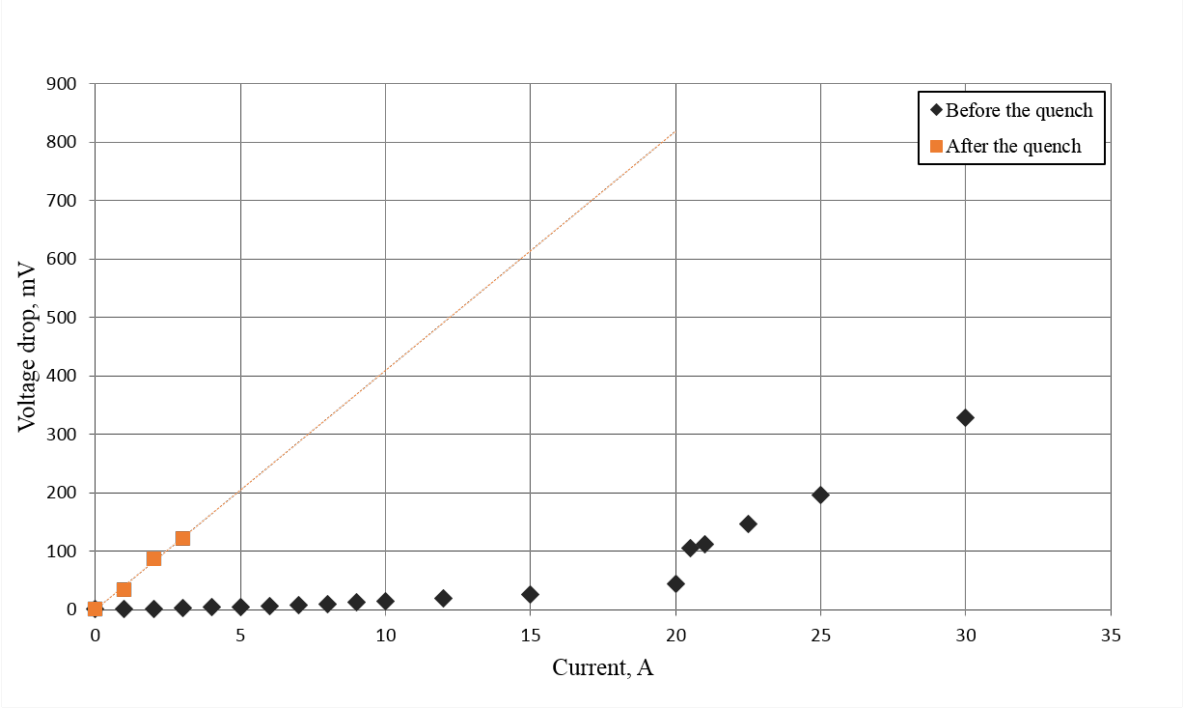

FIGURE 4: Current-Voltage characteristic of the magnet

ACKNOWLEDGMENTS

The authors are grateful to Wroclaw Networking and Supercomputing Center for granting access to the computing infrastructure.
The authors are grateful to Akademickie Centrum Cyfrowe Cyfronet AGH for granting access to the computing infrastructure.

REFERENCES

[1] T. Coombs, in *Superconductors in the Power Grid* (Elsevier, 2015), pp. 345–365.
[2] S. Kwak, S. Lee, S. Lee, W.-S. Kim, J.-K. Lee, C. Park, J. Bae, J.-B. Song, H. Lee, K. Choi, *et al.*, IEEE Transactions on Applied Superconductivity **19**, 1985–1988 (2009).
[3] K. Ding, T. Zhou, K. Lu, Q. Du, B. Li, S. Yu, X. Huang, C. Liu, K. Zhang, K. Jing, *et al.*, IEEE Transactions on Applied Superconductivity **28**, 1–4 (2017).
[4] L. Bromberg, M. Tekula, L. El-Guebaly, and R. Miller, Fusion Engineering and Design **54**, 167 – 180 (2001).
[5] K. Okuno, A. Shikov, and N. Koizumi, Journal of Nuclear Materials **329-333**, 141 – 147 (2004), proceedings of the 11th International Conference on Fusion Reactor Materials (ICFRM-11).
[6] Y. Guo, J. X. Jin, J. G. Zhu, and H. Y. Lu, IEEE transactions on applied superconductivity **17**, 2087–2090 (2007).
[7] K. Hamilton, A. E. Pantoja, J. G. Storey, Z. Jiang, R. A. Badcock, and C. W. Bumby, IEEE Transactions on Applied Superconductivity **28**, 1–5 (2018).
[8] M. Yoon, S. Lee, S. H. Park, J. Lee, G.-W. Hong, K. Choi, S. Hahn, S. Lee, J. H. Han, and W.-S. Kim, IEEE Transactions on Applied Superconductivity (2019).
[9] R. Gupta, M. Anerella, G. Ganetis, A. Ghosh, H. Kirk, R. Palmer, S. Plate, W. Sampson, Y. Shiroyanagi, P. Wanderer, *et al.*, IEEE Transactions on Applied Superconductivity **21**, 1884–1887 (2010).
[10] C. Senatore, M. Alessandrini, A. Lucarelli, R. Tediosi, D. Uglietti, and Y. Iwasa, Superconductor Science and Technology **27**, p. 103001 (2014).

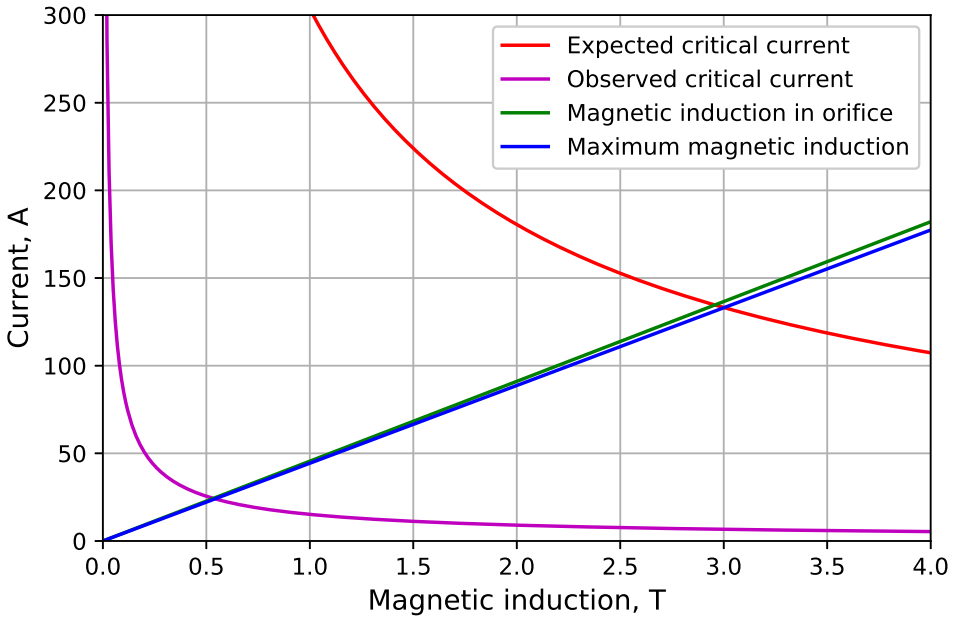

FIGURE 5: Expected and measured quenching behaviour of the solenoid

[11] S. Mukoyama, A. Nakai, H. Sakamoto, S. Matsumoto, G. Nishijima, M. Hamada, K. Saito, and Y. Miyoshi, "Superconducting joint of rebco wires for mri magnet," in *Journal of Physics: Conference Series*, Vol. 1054 (IOP Publishing, 2018) p. 012038.

[12] M. V. Silva Elipe, N. Donovan, R. Krull, D. Pooke, and K. L. Colson, Magnetic Resonance in Chemistry **56**, 817–825 (2018).

[13] M. A. Green, IEEE Transactions on Applied Superconductivity **28**, 1–5 (2018).

[14] J. Paasi, J. Lehtonen, T. Kalliohaka, and R. Mikkonen, Superconductor Science and Technology **13**, p. 949 (2000).

[15] H. Toriyama, Y. Fuchida, A. Nomoto, H. Taguchi, T. Takao, K. Nakamura, O. Tsukamoto, and M. Furuse, IEEE Transactions on Applied Superconductivity (2019).

[16] P. Skov-Hansen, Z. Han, and J. I. Bech, IEEE Transactions on applied superconductivity **9**, 2617–2620 (1999).

[17] W. Huang and J. Q. Chen, "Optimizing design of multi-coil solenoid hts magnet by pso algorithm," in *2018 IEEE International Conference on Applied Superconductivity and Electromagnetic Devices (ASEMD)* (IEEE, 2018), pp. 1–2.

[18] S. Kostromin, I. Meshkov, A. Sidorin, A. Smirnov, G. Trubnikov, and N. Shurkhno, Physics of Particles and Nuclei Letters **9**, 322–336 (2012).

[19] N. Agapov, D. Donets, V. Drobin, E. Kulikov, H. Malinovski, R. Pivin, A. Smirnov, Y. V. Prokofichev, G. Trubnikov, and G. Dorofeev, Physics of Particles and Nuclei Letters **9**, 422–424 (2012).

[20] C. Senatore, C. Barth, M. Bonura, M. Kulich, and G. Mondonico, Superconductor Science and Technology **29**, p. 014002 (2016).